Radiation Protection Dosimetry (2022), pp. 1–13 https://doi.org/10.1093/raddos/ncac005

ACTIVITY ESTIMATION WHEN DEALING WITH COLLECTIONS OF URANIFEROUS MINERALS

Luca Fedeli[1], Sandra Doria[2,3,*], Vanni Moggi Cecchi[4], Ilaria Cupparo[5,6], Lucilla Fabrizi[4,7] and Cesare Gori[8]

[1]S.O.C. Fisica Sanitaria Prato e Pistoia, Ospedale San Jacopo, Via Ciliegiole 51, 51100 Pistoia, Italy
[2]Istituto di Chimica dei Composti OrganoMetallici, Consiglio Nazionale delle Ricerche (ICCOM-CNR), Via Madonna del Piano 10, 50019 Sesto Fiorentino (FI), Italy
[3]European Laboratory For Non Linear Spectroscopy (LENS), Universitá degli Studi di Firenze, Via Nello Carrara 1, 50019 Sesto Fiorentino (FI), Italy
[4]Museo di Storia Naturale - Sistema Museale di Ateneo, Università degli Studi di Firenze, Via La Pira 4, 50121 Florence, Italy
[5]Dipartimento di Fisica, Universitá degli Studi di Firenze, Via Giovanni Sansone 1, 50019 Sesto Fiorentino (FI), Italy
[6]Scuola di Scienze della Salute Umana, Universitá degli Studi di Firenze, Largo Brambilla 3, 50134 Florence, Italy
[7]Dipartimento Scienze Terra, Università degli studi di Firenze, via La Pira 4, 50121 Florence, Italy
[8]Universitá degli Studi di Firenze, Piazza San Marco 4, 50121 Florence, Italy

*Correspondence to be sent to: e-mail: Corresponding author: doria@lens.unifi.it

Received 10 December 2021; revised 10 December 2021; editorial decision 6 January 2022; accepted 6 January 2022

The activity estimation of hand-size specimens of uraniferous minerals is not a trivial issue due to the manipulation difficulty caused by the emitted ionising radiation and the dependence of radiometric quantities from several parameters. Sample modelling requires approximations, leading to large uncertainty in the evaluation of the activity. In this work, a new procedure to evaluate uraniferous specimens activity, including a detailed description of measured parameters, the instrumentation and the mathematical formulation of the process, is presented. The proposed methodology takes into consideration sample size, ore composition and measured radiation. The procedure was used to measure the activity of a group of uraniferous mineral specimens belonging to Natural History Museum of the University of Florence, Italy. The experimental set-up was designed to reduce the measurement uncertainty. The aim of this work is to propose a methodology that can be easily applied to the specimens manipulation, conservation and exhibition.

INTRODUCTION

Uranium is one of the most 'dangerous' elements in social imaginary. This celebrity comes in large part from its use in nuclear weapons, in power plants and from nuclear and radiation accidents. From radiation protection point of view, literature about uranium mineral is focused on mining, processing industry, its use in energy and weapons production and waste management [(1–3)]. Despite its aura, uranium is a sought-after element from mineral's collectors. The best known species are Autunite, Vandenbrandeite, Uraninite, Uranophane, Uranocircite, Torbernite, Metatorbenite, Sklodowskite, Cuprosklodowskite, Becquerelite and Curite [(4–7)]; a comprehensive list of mineral species, subdivided into four classes according to their calculated radioactivity, has been provided by [(8)]. The specimens may show colours varying from grass green, emerald green, dark green, reddish orange and many others. They may be massive or may display crystals with various habits, from equant to needle shaped, sometimes well-developed, with sizes from millimetres to a few centimetres [(4)].

Several museums all around the world possess uranium minerals collections, with a number of samples varying from a few up to several tens. Radioprotection literature on these practices is very limited and focused on exposure levels [(9–16)]. Literature regarding the estimation of minerals activity is scarce and a significant set of samples has never been analysed in detail.

Uranium is a naturally occurring element with an average concentration of 2.8 parts per million in the Earth's crust, traces occur almost everywhere. Natural uranium is a mixture of three isotopes ^{234}U, ^{235}U and ^{238}U, together with their decay products, in the so-called *'secular equilibrium'*. A typical sample of natural uranium, almost all the mass (99.27%), consists of ^{238}U atoms. Less than 1% (about 0.72%) consists of ^{235}U atoms, and a very small amount (0.0054%) consists of ^{234}U atoms[(17–19)]. ^{238}U and ^{235}U are the parent nuclides of two independent decay series, while ^{234}U is a decay product of ^{238}U series and thus in *'secular equilibrium'* with its parent.

The proposed methodology allows to evaluate the sample activity through simple steps, considering few

parameters such as sample size, ore composition and emitted radiation. The novelty of this work concerns the development of procedure to measure uraniferous specimens activity, including a detailed description of measured quantities, used instrumentation and mathematical modellization of the process. Samples sizes vary from few to ten centimetres, implying the failure of the point-like source approximation; moreover, the self-absorption of minerals has to be considered in the activity evaluation. This effect may be relevant due to high attenuation of low-energy components of natural uranium gamma spectrum. Both effects (extended geometry and self absorption) have been considered in this work allowing an accurate estimation of the uranium mass in each mineral sample.

PROPOSED ACTIVITY ESTIMATION PROCEDURE

The activity of a radioactive material containing a radioisotope could in principle be calculated from the measurements of the dose rate D through the proportionality relation:

$$D = \Gamma \cdot A \tag{1}$$

where Γ is the specific gamma-ray dose constant[20, 21], i.e. the dose originated by a point source containing the unit activity of a radioisotope at the reference distance (d_{ref}) of 1 m. Γ is usually reported in literature in units of mSv/h/MBq @30 cm (or 1 m). However, quite often eq. (1) cannot be applied as it is and procedural arrangements are necessary. In particular, in the case under study most samples contain an insufficient amount of radioactivity to allow an accurate measurement of the corresponding dose rate through the reference instrument for such measurements (i.e. the ionisation chamber) because of its relatively low sensitivity. On the contrary, other radiation detectors, such as solid state scintillators or semiconductors, are characterised by single photon counting capabilities and therefore, by a much higher sensitivity, are sufficient for accurate detection of the radiation emitted even by low activity samples. Necessarily, when employing a single photon counting detector instead of an ionisation chamber a proper conversion factor K must be determined for the evaluation of the value of the dose D out from the signal S obtained with a single photon detector, usually expressed in terms of counts per second (cps).

Indeed this instrument *counts* only a fraction of the photons emitted from the source, therefore, in order to determine the activity, efficiency (ε) must be measured or calculated. The relation between efficiency and activity is

$$S = \varepsilon \cdot A. \tag{2}$$

Combining eq.(1) and (2), the efficiency can be calculated as

$$\varepsilon = \Gamma \cdot \frac{S}{D} = \frac{\Gamma}{K}, \tag{3}$$

where $K = D/S$ represents the counts-to-dose conversion factor, which can be calculated performing a measure with both spectrometer and ionising chamber on high-activity samples. The samples selected for this purpose were of different sizes and shapes. Using the above equations, activity can be calculated as

$$A = S \cdot \frac{K}{\Gamma}, \tag{4}$$

where S is the signal of the sample, measured with a spectrometer.

Further issues to be considered for the activity estimation is the possible failure of the point-source approximation, due to the non-negligible spatial extent of the samples with respect to the detector-to-source distance and due to the interaction of the emitted radiation within the sample itself. For these reasons the measured signal S requires a correction consisting in two main contributions: the geometric effect and the self-absorption. A detailed analysis is presented in the following section. To this purpose, a global correction factor F can be introduced, so that the final activity of a sample is given by (from eq.(4)):

$$A = S \cdot \frac{K}{\Gamma} \cdot F \tag{5}$$

In summary, the proposed measurements procedure to estimate the activity of the uriniferous samples consists in the following steps:

1. The radiation emitted from each sample is measured by means of a single photon counting detector.
2. The proper conversion factor K is estimated from concurrent measurements with ionisation chamber and single photon counting detector in the case of some selected high activity samples.
3. A correction factor F is computed for each sample to take into account geometric and self-absorption effects related to the specific geometry of that sample.
4. Finally, the activity estimate of each sample is obtained by including in eq.(5) the specific gamma-ray dose constant Γ of Uranium and all its daughters, assumed to be in secular equilibrium.

Measurements of the signal S

The gross signal T measured for each sample consists of two contributions: the actual signal S due to the radiation emitted from the sample and the background radiation B. The latter originates from the radiation sources present in the environment, the so-called natural background: radionuclides naturally occurring in the soil or in the construction materials and cosmic radiation. This contribution must be subtracted from T to properly calculate the sample activity:

$$S = T - B \tag{6}$$

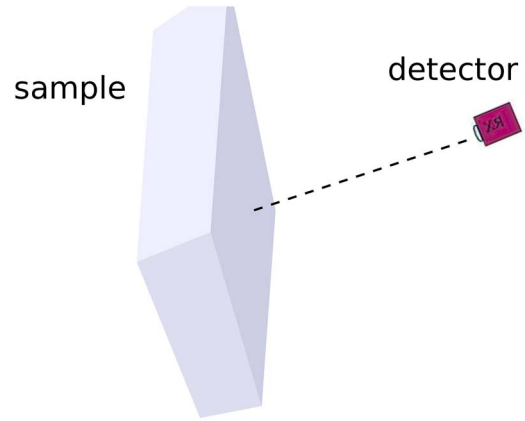

Figure 1. Geometric configuration of the measurements set-up optimised to reduce both extended source and self-absorption effects.

Calibration factor K

Some high-activity samples were chosen in order to be able to obtain reliable measurements in terms of dose rate by means of the ionisation chamber in addition to the ones in terms of cps by means of the solid state detector. For this goal, suitable samples from different mineral species were selected, considering different shape and size, in order to obtain an ensemble representative of the full collection. The factor K can then be evaluated as the average value of the ratio D/S_0 calculated over the whole set of selected samples. However, a preliminary verification is necessary: the self-adsorption of the emitted radiation produces an effect of beam hardening that is, even slightly, dependent on the physical dimensions of the sample, thus possibly making, in turn, the D/S_0 ratio dependent on the sample dimension. This possible effect must be verified and, in case, taken into account.

Specific gamma-ray dose constant Γ

The specific gamma-ray dose constant, as defined in eq. (1), was evaluated considering all the radionuclides present in the minerals, belonging to the ^{235}U and ^{238}U families, both assumed in secular equilibrium. The detailed derivation of the expression for the specific gamma-ray dose constant Γ is described in Appendix. In the end we obtained:

$$\Gamma_{Unat} = \Gamma_{F_{238}} + 0.0475 \cdot \Gamma_{F_{235}}, \tag{7}$$

where $\Gamma_{F_{238}}$ and $\Gamma_{F_{235}}$ include the contribution of all the radioisotopes daughters in secular equilibrium with their parents. The individual contributions are reported in literature for the majority of radioisotopes [22]. For few radioisotopes which are not tabulated in the above reference the specific gamma-ray dose constant was computed using the flux-to-dose conversion factor as a function of X-ray energy [23]. This process was peformed considering all radionuclides and, when available, the results were compared with literature; differences are of the order of few *per cent*.

Correction factor F

The assumption of point-source approximation leads to a possible misestimation of the activity that becomes non-negligible when dealing with samples thicker than a couple of cm. In addition, the radiation emitted inside a sample is partially absorbed by the sample itself before emerging from its outer face. The absorbed fraction depends on the radiation path length within the sample. Both extended source geometry and self-absorption effects can be somewhat reduced by placing the sample for the measurement in such a way that the thinner dimension is placed facing the detector (Figure 1); in this way, the variation in detector-to-source distance is minimised; also the length travelled by the radiation inside the sample is minimised. Nevertheless the self-absorption effect still remains significant as the prevalent effect leading to an underestimation of the activity. In the following text, we will estimate the contribution of both effects on the measured activity of the samples.

We now consider a point-like source of activity A with isotropic emission. In case of radiation emission at different energies, each characterised by an emission probability or *branching ratio* BR_i, the total signal S_P collected by the detector is expressed in terms of a weighted sum of the single-energy emissions:

$$S_P[cps] = \sum_i S_i(E_i) = \sum_i \varepsilon BR_i \cdot A, \tag{8}$$

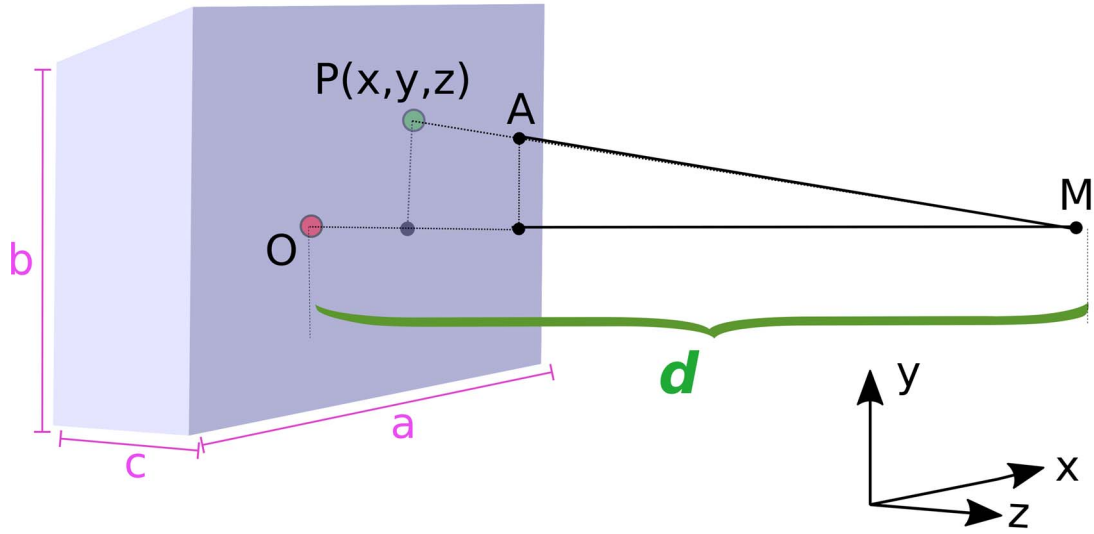

Figure 2. Schematic representation of an extended source of parallelepipedal shape: $P(x, y, z)$ is a generic emitting point within the source, M is the measurements position and A is the intersection of PM with outer face on the yz plane.

where ε is the mean value of the detector efficiency, which in general depends on the shape and material composition of the active volume of the detector, on the energy of the incident radiation and on the detector-to-source distance. In particular we consider:

$$\varepsilon(d) = \varepsilon(d_{ref})\frac{d_{ref}^2}{d^2}, \tag{9}$$

where d is the detector-to-source distance and d_{ref} is the reference distance used in efficiency (ε) calculation.

When we consider an extended source, the geometric effect can be taken into account using the inverse-square law applied to the detector-to-source distance for any emitting point of the source.

In a geometric approximation of the extended source with a parallelepipedal shape (Figure 2) the signal S_E (cps) collected by the detector located in the position M (Figure 2) is

$$\begin{aligned} S_E &= \int_V \sum_i \varepsilon BR_i \cdot \frac{d_{ref}^2}{\overline{PM}^2} \cdot A \cdot \frac{1}{V} dV \qquad (10) \\ &= \varepsilon A \sum_i BR_i \left[\int_{-\frac{a}{2}}^{\frac{a}{2}} dx \int_{-\frac{b}{2}}^{\frac{b}{2}} dy \int_{-\frac{c}{2}}^{\frac{c}{2}} dz \frac{d_{ref}^2}{\overline{PM}^2} \right] \frac{1}{V}, \end{aligned}$$

where the integral is calculated over the source volume $V = abc$ and $1/V$ is the normalisation factor. The ratio between eq.s (8) and (10) is the geometric contribution to the correction factor F.

Considering Figure 2, the radiation emitted from $P(x, y, z)$ travels a distance $\overline{PA}$ inside the source, where it experiences self-absorption. By including in eq. (10) the attenuation factor $T(E_i, \overline{PA})$, describing the fraction of radiation intensity absorbed, the following expression is obtained:

$$\begin{aligned} S_E = \varepsilon A \sum_i \cdot BR_i \cdot \\ \left[\int_{-\frac{a}{2}}^{\frac{a}{2}} dx \int_{-\frac{b}{2}}^{\frac{b}{2}} dy \int_{-\frac{c}{2}}^{\frac{c}{2}} dz \frac{d_{ref}^2}{\overline{PM}^2} T(E_i, \overline{PA}) \right] \frac{1}{V} \end{aligned} \tag{11}$$

As already stated, eq. (8) describes the signal S_P in the ideal case of a point source that must be corrected to include geometric effect and self-absorption. Therefore, the final correction factor F to be included in eq. (5) is given by

$$F = \frac{S_P}{S_E}. \tag{12}$$

The parameter in eq. 11 that needs to be calculated in quantitative terms is the attenuation fraction T. For each energy emission E_i, the radiation intensity is exponentially attenuated as it travels a distance x

Table 1. ***Chemical formula, density and molar weight of three selected components present in the uraniferous matrices.***

Samples	Chemical formula	ρ_C ($g\,cm^{-3}$)	Mmol ($g\,mol^{-1}$)
Enstatite	$Mg_2Si_2O_6$	3.2	202.2
Ferrosilite	$(Fe^{++}, Mg)_2Si_2O_6$	3.5	232.3
Wollastonite	$CaSiO_3$	2.9	116.2

inside the source according to the following relationship:

$$T(E_i, x) = e^{-\mu(E_i)\cdot x} = e^{-\left[\frac{\mu(E_i)}{\rho}\right]\cdot\rho\cdot x}, \quad (13)$$

where, in our case, $x = \overline{PA}$ (see Figure 2) and $[\frac{\mu(E)}{\rho}]$ is the mass attenuation coefficient which depends on the atomic species present in the source material and on its density. The attenuation coefficient is tabulated for a wide number of materials and for all elements in [24].

Since the sample is a composite of different atomic species (k), each characterised by its own attenuation coefficient $[\frac{\mu(E)}{\rho}]_k$, all of them must be taken into account in the calculation of the global attenuation coefficient of the sample. In addition, the actual density ρ_k of the atomic species k within any sample must be introduced. ρ_k can be inferred from the density ρ_C of the sample according to the following relationship: $\rho_k = \frac{Mmol(k)}{Mmol(C)}\rho_C$, where *Mmol* indicates the molar mass. Finally, the overall transmission factor T of the composite material is given by the product of the attenuation factors corresponding to each atomic species:

$$T(E_i, \overline{PA}) = \Pi_k \; e^{-\left[\frac{\mu(E_i)}{\rho}\right]_k\cdot\rho_k\cdot\overline{PA}} \quad (14)$$

If the mass attenuation coefficient of a composite material is not known *a prori*, as in our case, it is possible to compute it from its chemical composition by means of eq.(14). The mass attenuation coefficients of the single atomic species are available in ref. [24].

In Table 1 is presented the chemical formula and the parameters relevant for the determination of the mass attenuation coefficient in case of same common uraniferous samples.

In Figure 3, the mass attenuation coefficients, calculated according to eq. (14), are plotted in the energy range between 10 and 3 MeV for the three selected samples reported in Table 1. As noticeable, only below 150 keV, where the photoelectric effect is dominant, the differences are significative, while the three coefficients are almost coincident at higher energies. This means the low-energy part of spectrum is absorbed in the sample itself and the signal (S) is due in large part from emissions above 150 keV which are absorbed in the same way by all the considered samples. Since, to high extent, the actual energies of the emitted radiation are above 150 keV, the use of a unique value of the mass attenuation coefficient to compute the attenuation factor T for all the samples is reasonable. Therefore, we introduced in our calculation the value of the attenuation coefficient obtained by averaging the three curves shown in Figure 3. The overall geometric and self-absorption effect can then be gathered by computing S_E by introducing in eq. (11) the attenuation factor T of eq. (14).

In order to better visualise the impact of extended source correction with respect to the point source with the same activity, spectral simulations of natural uranium emission were performed, assuming both families of the isotopes ^{238}U and ^{235}U in secular equilibrium and natural abundance. The simulation, reported in Figure 4, is referred to the case of a point source (blue line) and of an extended sample (red line) with dimensions typical of the samples under investigation, of equal activity. In agreement with the trend of the mass attenuation coefficient shown in Figure 3, the emission energies below 150 KeV are strongly attenuated, while the higher energy spectral components (above 150 keV) are only mildly attenuated.

Numerical values of extended source and self-absorption correction (F factor) are reported in Figure 5 as a function of the sample thinner dimension (c size); the other dimensions (i.e. a and b) are set to 1.5 c, in particular considering sizes larger than 1.5 cm the dependence of F factor with c size is approximately linear.

Detection Limit

In measurement processes when the measured signal is *'similar'* to the background it is difficult to distinguish between signal and background. This effect is characterised with two different quantities: the *Decision Threshold* (DT) and the *Detection Level* (DL)[25, 26]. The first represents the threshold above which the

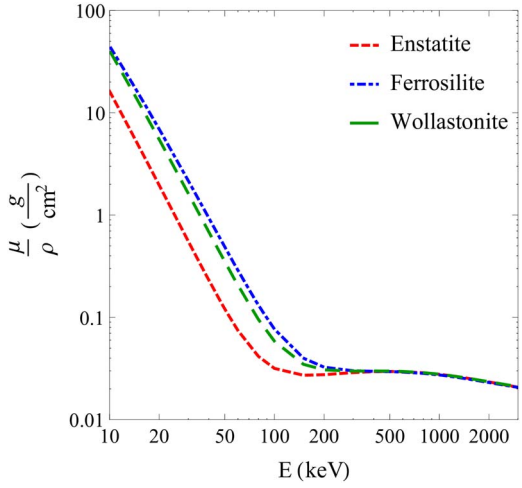

Figure 3. Mass attenuation coefficient as a function of energy for three selected samples of the collection.

measure is statistically different from the background but the signal is too close to background and only a qualitative analysis is possible (i.e. '*there is something, but is no possible to evaluate the correct magnitude*'). The latter is the value above which a quantitative measure of activity is reliable (i.e. '*there is something and the best activity estimation is...*'). These values depend from the uncertainty on the measured parameters (i.e. on S, F, K, Γ, etc..). In the proposed procedure, DL, determined following [25], is used as lower value below which it is not possible to evaluate the sample activity.

EXPERIMENTAL APPLICATION OF THE PROPOSED METHOD TO THE CONSIDERED COLLECTION OF URANIFEROUS MINERALS

We applied the method for the calculation of the activity of uraniferous minerals described in the previous chapter to a collection of radioactive minerals belonging to the Mineralogical and Lithological Collection of the Natural History Museum, University of Florence, Italy (https://www.sma.unifi.it/vp-356-mineralogy-and-lithology.html?newlang=eng). The whole collection counts 361 uraniferous samples of different mineral composition. A picture of few samples is reported in Figure 6. According to the procedure reported in the first section of this guide, as a first step the intensity of the radiation output of each sample of the collection was measured by means of portable gamma-ray spectrometer FLIR System (ICx Technologies) equipped with a 1.5 "x 1.5" NaI(Tl) detector. The lower threshold of the window of the spectrometer was set to 5 keV and the upper one to 2.8 MeV in order to make the detector sensitive to the whole spectrum of natural uranium emission. The detector-to-source distance (d) was set to 30 cm as a balance between decreasing detector efficiency with distance and increasing likelihood of the geometric approximation of the investigated sample to a point source. In addition, with increasing distance a reduction of the error due to sample mispositioning is also attained. The experimental set-up is sketched in Figure 7.

Signal and background measurements

The signal measurements were performed by employing the portable gamma-ray spectrometer FLIR System (ICx Technologies). As discussed in section 'Measurements of the signal S', the count rate (T) measured with the detector is the sum of two contributions: the signal emitted from the sample (S) and the background radiation (B). This latter contribution must be subtracted from T to properly determine the activity of the radioactive minerals. The signal S from the sample is then:

$$S = T - B \tag{15}$$

The background measurement was performed several times during each measuring session (204 values in total). No relevant differences were reported from one session to another. Mean and standard error were used to characterise background radiation:

$$B = (132.7 \pm 0.8)\ \text{cps} \tag{16}$$

Evaluation of the conversion factor K

Dose rate measurements necessary for the calculation of the conversion factor K (according to eq.(4)), i.e. the correspondence between dose rate and cps, were performed by replacing the solid state NaI(Tl) detector with an ionisation chamber (Fluke Biomedical 451B) positioned in such a way that the centre of the sensitive volume of the ionisation chamber was located at the same distance from the sample as the centre of the NaI(Tl) detector. These couples of measurements were repeated for 88 different samples specifically selected from the collection because of their higher activity in order to better estimate mean value and standard error on the parameter K. The result was:

$$K = (1.808 \pm 0.026)\ \frac{\text{nSv}}{\text{h} \cdot \text{cps}} \tag{17}$$

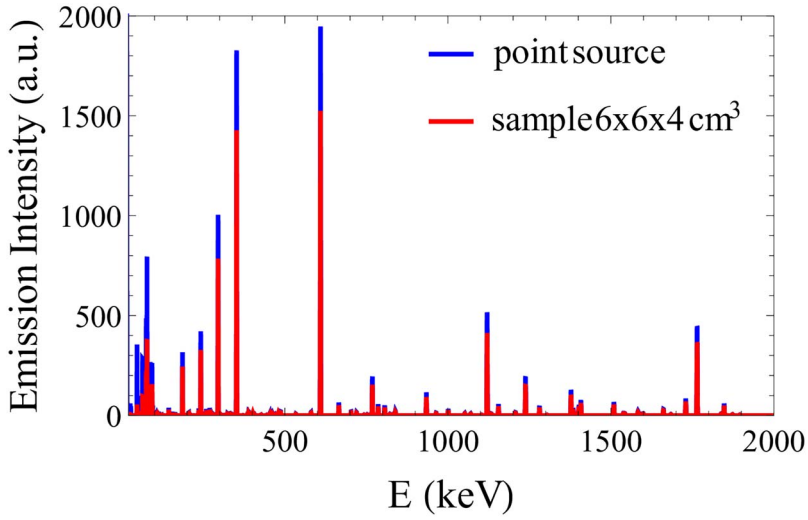

Figure 4. Simulated emission spectra of a point source (blue line) and of an extended source of size 7x6x6 cm^3 (blue line). In the latter case geometric effect due to self-absorption was quantified.

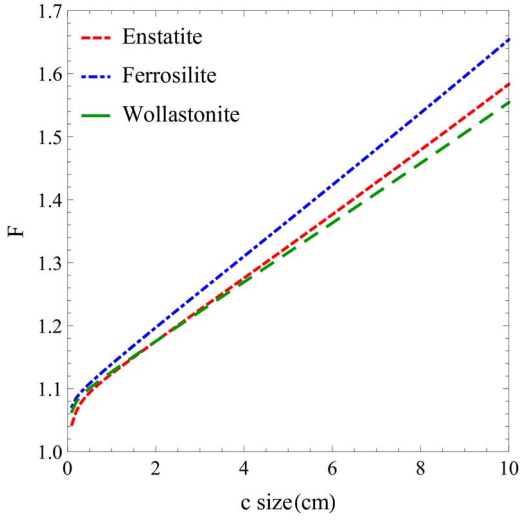

Figure 5. F factor as a function of c sample size, considering $a = b = 1.5\ c$.

In principle, the different size of the samples could affect the determination of K, due to the different self-absorption of the emitted radiation and the possible consequent different modification of the energy spectrum of the radiation escaping from the samples and impinging on the detectors. Actually, the efficiency of both detectors (mainly one of the solid state detectors) depends on the radiation energy. In order to evaluate this effect, the value of K was plotted as a function of the samples volume as reported in Figure 8. The scatter plot shows no appreciable dependence (with 95% CL) between sample size and K value.

Evaluation of the correction factor F

The evaluation of the factor F was performed following the procedure described in section 'Correction factor F', under the assumption of secular equilibrium of the two isotopic families with parents ^{238}U and ^{235}U and considering the isotopic composition of natural uranium equal to 99.3% and 0.7% for ^{238}U and ^{235}U, respectively. An *ad hoc* software was developed using the programming language *Mathematica* (*Wolfram Research, Champaign IL, USA*) to evaluate geometric effect and self-absorption contributions to the correction factor F for each sample.

The geometric effect leads to a slight overestimation of the activity of the order of a few percent (values range from 1% to 4% for samples thickness from 3 to 10 cm). The geometric correction becomes negligible for small size samples (thickness << detector-to-source distance). On the other hand, the self-absorption produces a significant underestimation of the samples activity. In eq. (5) the two contributions are combined together. Calculations lead to values of F ranging between 1.14 and 1.59, depending on the samples size. The uncertainty on F was computed as described in the 'Uncertainty evaluation' section.

Calculation of Γ

The calculation of the specific gamma ray constant Γ for natural uranium has been carried out as described

Figure 6. Picture of three samples of the mineral collection of the University of Florence Natural History Museum (Inv. N^o G47197, G47214, G47221).

Table 2. ***Estimated activity and main characteristics of three selected samples of the collections.***

Sample	**Species**	**^{238}U Activity (MBq)**	**Size (cm^3)**	**m_{238} (g)**
a)	Cuprosklodowskite	1.17 ± 0.10	7, 6, 6	94.36
b)	Vandenbrandeite	0.32 ± 0.04	7, 6, 5	25.85
c)	Metatorbernite	0.117 ± 0.013	7, 5, 4	9.44

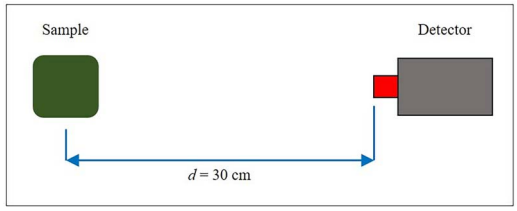

Figure 7. Picture of experimental set-up: a distance of $d = d_{ref} = 30$ cm was set between the detector and the centre of the sample.

in section 'Specific gamma-ray dose constant Γ' and is extensively reported in Appendix. The result for natural uranium, in case of d_{ref} =30 cm as reference distance (Γ scales with inverse square law of distance from source) is

$$\Gamma_{U_{nat}} = (3.02 \pm 0.06)\ \frac{\mu\text{Sv}}{\text{h} \cdot \text{MBq}}\ @\ 30\ \text{cm} \qquad (18)$$

Activity estimation and detection limit

The activity for each sample of the collection can be computed from the parameters listed in Table 3, following the procedure described in the first section of this guide. Following ([25]), we also evaluated the Detection Limit (DL) of the activity (assuming normal distributions) with a confidence level of 95%:

$$DL = 250\ \ \text{Bq}\ \ \text{of}\ \ ^{238}\text{U} \qquad (19)$$

Table 3. ***Parameters used for the minerals activity estimation and their uncertainty. The error on the variable S and T depends also from the measurement time (see also the 'Uncertainty evaluation' section.***

Symbol	**Value**	**Uncertainty**
K	$1.81 \pm 0.03\ \frac{\text{nSv}}{\text{h}\cdot\text{cps}}$	1.4%
Γ	$3.02 \pm 0.06\ \frac{\mu\text{Sv}}{\text{h}\cdot\text{MBq}}$ @ 30 cm	2%
F	from 1.14 to 1.59	∼3.6%*
d	30 ± 1 cm	3.3%
B	132.7 ± 0.8 cps	0.7%
T	from 150 to 3000 cps	∼2%*
S	from 15 to 3000 cps	∼2%*

This means that lower values of activity cannot be measured. As an example of our results, in Table 2 is reported the estimated activity of the three samples depicted in Figure 6 that were selected as representative of the collection in terms of different activity and different mineralogical species. Their approximate size is also reported in the table.

Uncertainty evaluation

Uncertainty evaluation represents an important aspect of any measurement: for this reason the uncertainty in the activity evaluation of the samples of our collection is reported here with some details. Actually, the error on the calculation of the activity depends on a combination of the errors affecting each

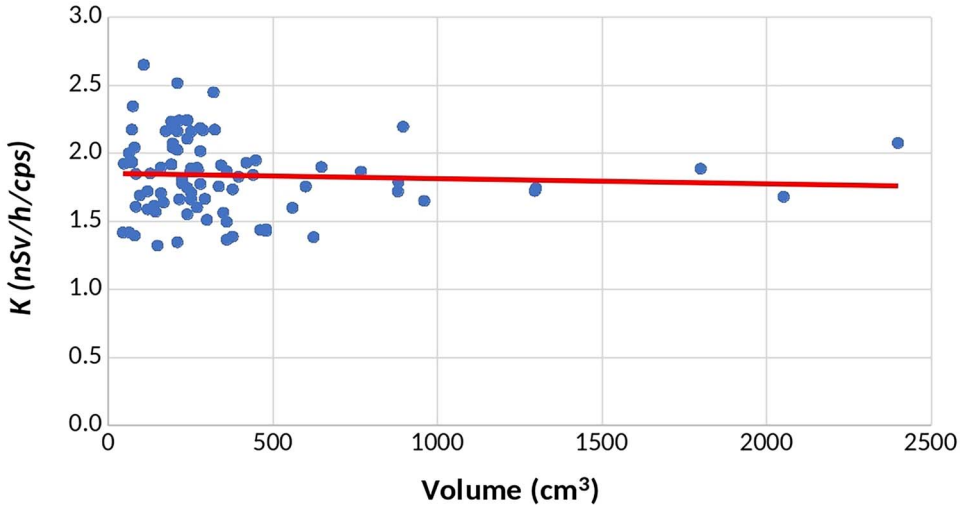

Figure 8. K factor as a function of samples volume; the linear fit is shown in red, showing no appreciable dependence with minerals size.

one of the parameters necessary for its calculation. Therefore, the uncertainty affecting each parameter will be addressed. The ones taken into account are listed below.

Source signal S

As previously stated, several background measurements were performed during the measuring sessions and uncertainty on B was chosen equal to the standard error of the measured values, that is, 0.8 cps.

A single measure of T was performed for each sample. In this case the uncertainty can be evaluated considering statistical fluctuations associated with discrete measure described by Poisson statistics (the standard deviation is the square root of the number of counts). The final uncertainty on the source signal ($S = T - B$), expressed as counts per second (cps), can be calculated as:

$$\Delta S = \sqrt{\Delta T^2 + \Delta B^2} \tag{20}$$

Since the activity of the various samples is quite different, the duration of each measurement, t, was longer for low activity samples in order to improve the counting statistics. Labelling with C_t the counts detected in the measurement time t, $T = C_t/t$, where the error on t is negligible as it is electronically determined, and

$$\Delta T = \frac{\Delta C_t}{t} = \frac{\sqrt{C_t}}{t} = \sqrt{\frac{T}{t}}, \tag{21}$$

where $\sqrt{C_t}$ is the uncertain on C_t assuming a Poisson statistic distribution. The uncertainty on S can be calculated combining eq.(21) and (20):

$$\Delta S = \sqrt{\frac{T}{t} + \Delta B^2} = \sqrt{\frac{T}{t} + 0.8^2} \tag{22}$$

Typical T values ranges are between 150 and 3000 cps and $t \simeq 15$ s. ΔS results are around 2%, with maximum values near to 20% in case of low activities (close to DL).

Detector-to-source distance (d)

As mentioned in section 'Signal and background measurements', the selected sample-to-detector distance, d, was 30 cm. The uncertainty on this variable derives from the irregular sizes of the samples and from samples positioning errors. Assuming an uncertainty of 1 cm, as the error standard deviation, $\Delta d \sim 3.3\%$.

Conversion coefficient K

Uncertainty on the counts-to-dose conversion factor K was set as the standard deviation of the whole set of measurement performed (see section 'Calibration factor K'), resulting in a relative error of 1.4%.

Specific gamma ray dose constant Γ

Uncertainty on the specific gamma-ray dose constant Γ can be evaluated by comparing the Γ values calculated as described in Appendix for the most relevant radioisotopes daughter of ^{238}U and ^{235}U with the corresponding values reported in literature [22]. The differences are of the order of 2% and this value is assumed as the uncertainty on Γ.

Correction coefficient F

The error on the correction coefficient F arises from two independent sources of uncertainty: the first one relating to the uncertainty on the actual dimensions of the sample, i.e. ΔF_{Vol} and the second relating to the uncertainty on the mineral sample composition, that is, on its actual attenuation coefficient, i.e. $\Delta F_{Mineral}$. In Figure 5 we reported the variation of the calculated F factor as a function of the size c, the dimension of the sample along the sample-detector line, assuming the other two dimensions, a and b, both equal to a 1.5 c. The uncertainty on the measured dimensions of the sample (Δ) is assumed to be 0.5 cm. The error ΔF_{Vol} can be evaluated as a function of the sample dimensions through the following relationship:

$$\begin{aligned}\Delta F_{Vol}^2 &= \left[\frac{F(a\pm\Delta,b,c)}{F(a,b,c)}-1\right]^2+\\ &+\left[\frac{F(a,b\pm\Delta,c)}{F(a,b,c)}-1\right]^2+\\ &+\left[\frac{F(a,b,c\pm\Delta)}{F(a,b,c)}-1\right]^2 \qquad (23)\end{aligned}$$

In Figure 9, a plot of such calculation is reported, considering Ferrosilite, Enstatite and Wollanstonite. Considering a sample of a 'normal' size 6x6x4 cm^3, ΔF_{Vol} is about 2%. As previously stated different chemical compositions may lead to different attenuation coefficients and thus to different self-absorption. This effect on the calculation of F is evident from Figure 5. Differences on mineral composition affect the calculation of F in a non-negligible way. Considering again Figure 5, for a sample of a 'normal' size 6x6x4 cm^3, $\Delta F_{Mineral}$ is about 3%. The total uncertainty on factor F (which includes both self-absorption and sample size) can be determined as the square sum of the errors on the mineral volume estimation ΔF_{Vol} and on the chemical composition $\Delta F_{Mineral}$, which we estimated to be of the order of 2% and 3%, respectively:

$$\begin{aligned}\Delta F &= \sqrt{\Delta F_{Vol}^2+\Delta F_{Mineral}^2}\simeq\\ &\simeq \sqrt{2\%^2+3\%^2}\simeq 3.6\% \qquad (24)\end{aligned}$$

Total uncertainty on the activity A

The uncertainty on each sample activity was evaluated *ad hoc*, considering the specific sizes and the measured signal as described above. A summary of uncertainty evaluation of the quantities just addressed is reported in Table 3. The total uncertainty

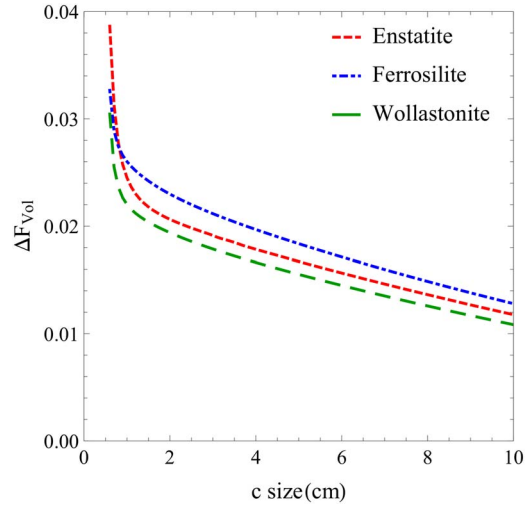

Figure 9. ΔF_{Vol} as a function of c samples size, considering $a = b = 1.5\ c$.

on activity can be finally calculated as the squared sum of the values on each parameter:

$$\Delta A = \sqrt{\Delta S^2 + (2\cdot\Delta d)^2 + \Delta F^2 + \Delta\Gamma^2 + \Delta K^2} \qquad (25)$$

This led to an uncertainty range between 7.5 and 20% with mean value of 8.2%. Larger values are generally for low activity samples, smaller values for high activity levels.

CONCLUSIONS

In this work a well-defined procedure for activity estimation of uraniferous minerals, based on radiometric measurements, was proposed. All the steps of the procedure were carefully planned to maximise the accuracy of the final activity assessment and minimise both uncertainties and systematic errors. Samples sizes lead to failure of the point-source approximation; therefore, proposed methodology was developed to consider non-trivial aspects such as geometric and self-absorption effects.

The procedure was applied to a collection of 361 uraniferous minerals. *In situ* measurements were carried out using both ionisation chamber and NaI portable spectrometer, calibrated by an accredited laboratory. Extended source effects were minimised using *ad hoc* measuring geometry and appropriate correction factors were computed for each sample by including ore composition and gamma-ray dose constant, computed assuming natural Uranium in secular equilibrium with all its daughters.

There are two elements of novelty in this work with respect to previous literature. One is the simplicity

of the proposed procedure, which can be applied to different minerals collection, performing *in situ* measurements with no need for mineral destruction or transport to a specialised laboratory. The other is the large number of samples measured using the proposed methodology.

The results shown in present *guide* can be used both from public and private collections of uraniferous ore to correctly manipulate, stock and exhibit own minerals. In forthcoming studies we will consider further radioprotection issues such as workers and public' exposure, manipulation warnings and gas radon concentration estimation.

ACKNOWLEDGEMENT

The authors thank Giorgio Scali for providing the pictures of the minerals reported in this paper.

REFERENCES

1. IAEA. *Occupational Radiation Protection in the Uranium Mining and Processing Industry*. In: Number 100 in Safety Reports Series. International Atomic Energy Agency. (Vienna) (2020).
2. Gaso, M. I., Segovia, N. and Morton, O. *Environmental impact assessment of uranium ore mining and radioactive waste around a storage centre from Mexico*. Radioprotection **40**, S739–S745 (2005).
3. Duport, P. *Radiation Protection in Uranium Mining: Two Challenges*. Rad Prot Dosim **53**(1-4), 13–19 (1994).
4. Anthony, J. W., Bideaux, R. A., Bladh, K. W. and Nichols, M. C. Handbook of Mineralogy, Volume IV. Arsenates, Phosphates, Vanadates. (Tucson, AZ: Mineral Data Publishing) (2000).
5. Friedman, H. Minerals guide. (1997-2021). https://www.minerals.net/Minerals/A.aspx.
6. Vaes, J. F. and Guillemin, C. *Minéraux d'uranium du Haut-Katanga*. Bulletin de Minéralogie **1**, 167–168 (1958).
7. Schoep, A. *La sklodowskite, nouveau mineral radioactif*. C. R. Acad. Sci. Paris **179**(143) (1924).
8. Barthelmy, D. Webmineral database. (1997-2014).
9. Freedman, J. *Storage of the Radioactive Mineral Collections at Plymouth City Museum and Art Gallery*. UK. Collections **7**(2), 201–212 (2011).
10. Lopes, F., Ruivo, A., Muralha, V. S. F., Lima, A., Duarte, P., Paiva, I., Trindade, R. and de Matos, A. P. *Uranium glass in museum collections*. J. Cult. Herit. **9**, e64–e68 (2008).
11. Rowe, S. *Managing Small Radioactive Collections in the UK: Experiences from the Polar Museum*. Cambridge. J Conserv Mus Stud **16**(1), 4 (2018).
12. Rowan, A. Here be Dragons: The Care and Feeding of Radioactive Mineral Species. (2017). https://www.academia.edu/31501150/Here_be_Dragons_The_Care_and_Feeding_of_Radioactive_Mineral_Species_Feb_2017_.
13. Rowan, A. Here be Dragons: The Care and Feeding of Radioactive Mineral Species – Mineral Data. (2017). https://www.academia.edu/31507928/Here_be_Dragons_The_Care_and_Feeding_of_Radioactive_Mineral_Species_Mineral_Data_Feb_2017_.
14. Commission de Recherche et d'Information Indépendantes sur la radioactivité. Risques liés á la détention de minéraux radioactifs. Fiche CRIIRAD N°16–30, (2016). https://www.criirad.org/objets-radioactifs/16-30mineraux%20radioactifs.pdf.
15. Institut de Radioprotection et de surete nucleaire. Mineraux radioactive, introduction. (2016). https://www.irsn.fr/FR/connaissances/Environnement/expertises-locales/gestion-sources-radioactives/mineraux-radioactifs/Pages/sommaire-mineraux-radioactifs.aspx#.Yf1JJPnMKUk.
16. Boisson, J. M. and Leydet, J. C. L'uranium et ses descendants; la radioactivité in La radioactivité et les Minéraux Uraniféres Français. (Editions du piat, Yssingeaux: Le Régne Minéral Hors-Série) (1998).
17. Chernyshev, I. V., Golubev, V. N., Chugaev, A. V. and Baranova, A. N. *238U/235U isotope ratio variations in minerals from hydrothermal uranium deposits*. Geochem. Int. **52**, 1013–1029 (2014).
18. F.E Senftle, Lorin Stieff, Frank Cuttitta, and P.K Kuroda. *Comparison of the isotopic abundance of U235 and U238 and the radium activity ratios in Colorado Plateau uranium ores*. Geochim. Cosmochim. Acta, **11**(3),189–193 (1957).
19. Cowan, G. A. and Adler, H. H. *The variability of the natural abundance of 235U*. Geochim. Cosmochim. Acta **40**(12), 1487–1490 (1976).
20. Unger, L. M. and Trubey, D. K. Specific Gamma-Ray Dose Constants for Nuclides Important to Dosimetry and Radiological Assessment (ORNL/RSIC–45/Rev1). Technical report. (Oak Ridge National Lab., TN (USA)) (1981).
21. Battat, M. E. and (Chairman) ANS-6.1.1 Working Group. *American National Standard Neutron and Gamma-Ray Flux-to-Dose Rate Factors*. In: Technical report, ANSI/ANS-6.1.1-1977 (N666). (LaGrange Park, Illinois: American Nuclear Society) (1977).
22. Delacroix, D., Guerre, J. P., Leblanc, P. and Hickman, C. *Radionuclide and Radiation Protection Data Handbook 2002*. Rad Prot Dosim **98**(1), 1–168 (2002).
23. Smith, J. H. Flux To Dose Rate Conversion Factors for Gamma Ray Exposure. NASA Technical report No. 32-439. (Technical report, Jet Propulsion Laboratory) (1963).
24. NIST. *X-Ray Mass Attenuation Coefficients*. NIST Standard Reference Database 126 (1996-2004).
25. Currie, L. A. *Limits for qualitative detection and quantitative determination*. Application to radiochemistry. Analytical Chemistry **40**(3), 586–593 (1968).
26. BIPM. Evaluation of measurement data - Guide to the expression of uncertainty in measurement. (JCGM, France metrological insitute) 100 (2008). https://www.bipm.org/documents/20126/2071204/JCGM_100_2008_E.pdf/cb0ef43f-baa5-11cf-3f85-4dcd86f77bd6.

APPENDIX: COMPUTATION OF THE SPECIFIC GAMMA-RAY DOSE CONSTANT OF NATURAL URANIUM

The determination of the specific gamma-ray dose constant of natural uranium depends on the relative mass abundances of the two isotopes (^{238}U and ^{235}U) and on their specific activities (activity per unit mass). Considering natural uranium, were both isotopes are in secular equilibrium with their daughters (i.e. the activity of each isotopes is the same as of his parent), the total activity can be calculated as:

$$A_U = A_{F_{235}} + A_{F_{238}} = F_{235}A_{235} + F_{238}A_{238} \tag{A1}$$

were $A_{F_{235}}$ and $A_{F_{238}}$ are the total activities of the two families (i.e. the sum of the activity of all nuclides in each family) and A_{235} (A_{235}) is the activity of isotope ^{235}U (^{238}U). F_{235} and F_{238} are the number of daughters in each family (11 and 14 respectively for ^{235}U and ^{238}U). The total specific gamma-ray dose constant Γ_U can be calculated considering the contribute of each isotopes of each family:

$$\begin{aligned}\Gamma_U A_U &= \sum_{i=1}^{F_{235}} \Gamma_i \cdot A_i + \sum_{i=1}^{F_{238}} \Gamma_i \cdot A_i \\ &= A_{235} \cdot \sum_{i=1}^{F_{235}} \Gamma_i + A_{238} \cdot \sum_{i=1}^{F_{238}} \Gamma_i \\ &= \Gamma_{F_{235}} \cdot A_{235} + \Gamma_{F_{238}} \cdot A_{238} \\ &= \frac{\Gamma_{F_{235}}}{F_{235}} \cdot A_{F_{235}} + \frac{\Gamma_{F_{238}}}{F_{238}} \cdot A_{F_{238}}\end{aligned} \tag{A2}$$

$\Gamma_{F_{238}}$ and $\Gamma_{F_{235}}$ are the sum of gamma constants of each nuclide respectively in ^{235}U and ^{238}U family. Gamma constant was calculate by including eq.(A1) in eq.(A2)

$$\begin{aligned}\Gamma_U &= \frac{\Gamma_{F_{235}} \cdot A_{235} + \Gamma_{F_{238}} \cdot A_{238}}{F_{235}A_{235} + F_{238}A_{238}} \\ &= \frac{\Gamma_{F_{238}} + \Gamma_{F_{235}} \cdot \alpha}{F_{238} + F_{235} \cdot \alpha}\end{aligned} \tag{A3}$$

where α is the ratio between activity of ^{235}U and ^{238}U (i.e. $\alpha = A_{235}/A_{238}$). In measurement procedure described above, the activity of ^{238}U is used as reference instead of A_U, thus eq.(A2) become

$$\begin{aligned}\Gamma_{Unat} A_{238} &= \Gamma_{F_{235}} \cdot A_{235} + \Gamma_{F_{238}} \cdot A_{238} \\ \Gamma_{Unat} &= \Gamma_{F_{238}} + \Gamma_{F_{235}} \cdot \alpha\end{aligned} \tag{A4}$$

Γ_{Unat} represents the gamma constant of natural uranium referred to activity of ^{238}U isotope. Activity can be calculated considering the decay constant λ and the natural abundance of two families

$$\begin{aligned}A_{235} &= \lambda_{235} N_{235} = \lambda_{235} \frac{m_{235}}{Mmol_{235}} N_0 \\ A_{238} &= \lambda_{238} N_{238} = \lambda_{238} \frac{m_{238}}{Mmol_{238}} N_0\end{aligned} \tag{A5}$$

where m_{235} (m_{238}) is the mass of the isotope 235 (238) contained in the sample, *Mmol* is the molar mass of the isotope (i.e. 235 g/mol and 238 g/mol) and N_0 is the Avogadro's constant. The α parameter can be calculated as

$$\begin{aligned}\alpha &= \frac{A_{235}}{A_{238}} = \frac{\lambda_{235} \frac{m_{235}}{Mmol_{235}} N_0}{\lambda_{238} \frac{m_{238}}{Mmol_{238}} N_0} \\ &= \frac{\lambda_{235}}{\lambda_{238}} \cdot \frac{m_{235}}{m_{238}} \cdot \frac{Mmol_{238}}{Mmol_{235}}\end{aligned} \tag{A6}$$

The mass ratio of the two isotopes and their decay probability are [(1)]

$$\frac{m_{235}}{m_{238}} = \frac{0.007}{0.993}$$

$$\lambda_{238} = \frac{ln(2)}{4.51 \cdot 10^9 y}$$

$$\lambda_{235} = \frac{ln(2)}{7.04 \cdot 10^8 y}$$

which can be included in eq.(A6)

$$\begin{aligned}\alpha &= \frac{4.51 \cdot 10^9}{7.04 \cdot 10^8} \cdot \frac{0.007}{0.993} \cdot \frac{238}{235} \\ &= 6.406 \cdot 0.00705 \cdot 1.0127 = 0.0457\end{aligned} \tag{A7}$$

substituting numerical values in eqs.(A1), (A3) and (A4)

$$A_U = (F_{238} + F_{235} \cdot \alpha) \cdot A_{238} = 14.503 \cdot A_{238} \tag{A8}$$

$$\Gamma_U = 0.0690 \cdot \Gamma_{F_{238}} + 0.00315 \cdot \Gamma_{F_{238}}$$

$$= 0.208 \ \frac{\mu\text{Sv}}{\text{h} \cdot \text{MBq}} \ @ \ 30\text{cm} \tag{A9}$$

$$\Gamma_{Unat} = \Gamma_{F_{238}} + 0.0457 \cdot \Gamma_{F_{238}}$$

$$= 3.023 \ \frac{\mu\text{Sv}}{\text{h} \cdot \text{MBq}} \ @ \ 30\text{cm} \tag{A10}$$

the ratio between Γ_{Unat} and Γ_U is exactly the ratio between A_U and A_{238} (i.e. $\Gamma_{Unat} A_{238} = \Gamma_U A_U$).

REFERENCES

1. M.M. Be, Ch. Dulieu, and V. Chiste. *NUCLEIDE-LARA, a library for alpha, X and gamma emissions sorted by increasing energy (CEA-R-6201)* (2008).